

## Design, synthesis, and in vivo evaluation of oxamniquine methacrylate and acrylamide prodrugs

Roberto Parise Filho,<sup>a,\*</sup> Carla Maria de Souza Menezes,<sup>a</sup> Pedro Luiz Silva Pinto,<sup>b</sup> Gilberto Alvarenga Paula,<sup>d</sup> Carlos Alberto Brandt<sup>c</sup> and Maria Amélia Barata da Silveira<sup>a</sup>

<sup>a</sup>Department of Pharmacy, Faculty of Pharmaceutical Sciences, University of São Paulo, Av. Prof. Lineu Prestes, 580, ZIP 05508-900 São Paulo, Brazil

<sup>b</sup>Schistosomiais Sector, Adolfo Lutz Institute, Av. Dr. Arnaldo, 355, ZIP 01246-902 São Paulo, Brazil

<sup>c</sup>Butantan Institute, Av. Vital Brazil, 1500, ZIP 05503-900 São Paulo, Brazil

<sup>d</sup>Department of Statistics, Institute of Mathematics and Statistics, University of São Paulo, Rua do Matão, 1010, ZIP 05508-090 São Paulo, Brazil

Received 10 October 2005; revised 3 November 2006; accepted 13 November 2006  
Available online 16 November 2006

**Abstract**—Oxamniquine is an antiparasitic agent commonly used in therapeutics against *Schistosoma mansoni*. Although it is well tolerated, some adverse effects justify the search for new compounds with prolonged biological action, so that monomeric and polymeric oxamniquine prodrugs were designed. Synthetic results assisted by molecular modeling study showed the possibility to obtain the corresponding monomeric forms of the oxamniquine methacrylate (1) and oxamniquine acrylamide (2). Successful copolymerization procedure only occurred on the methacrylic compound, generating the oxamniquine methacrylate copolymer (3). Submitted to a preliminary in vivo biological evaluation, a similar oxamniquine profile was observed to the monomeric forms although an inadequate drug release may be responsible for the methacrylic copolymer failure.

© 2006 Elsevier Ltd. All rights reserved.

### 1. Introduction

Schistosomiasis, an illness which has been affecting humanity since primordial times, is one of the most relevant parasitic diseases present in underdeveloped countries. Even after great advances in treatment and prevention, the disease still shows significant values of prevalence and morbidity.<sup>1</sup> It is estimated that 200 million people have been infected and 600 million are at risk of contracting the infection.<sup>2,3</sup> Schistosomiasis is responsible for almost 500,000 deaths each year. Urinary schistosomiasis causes either bladder cancer or renal insufficiency, while the intestinal form is related to hepatic fibroses and portal hypertension.<sup>1</sup>

Although the control activities seem to be well elaborated, they have been shown to be inefficient. As multiple

factors are involved, a real promise of a definitive and sustainable cure cannot yet be offered,<sup>4</sup> which makes chemotherapy play an important and crucial role to prevent, suppress, and treat the illness.<sup>2,5,6</sup>

Oxamniquine is a schistosomicide agent widely used in Brazilian therapeutics against *Schistosoma mansoni* due to its low cost and good efficacy. Although the drug is relatively well tolerated, some adverse effects in the central nervous system, including convulsions and hallucinations, have been reported.<sup>1,7,8</sup> As a consequence, new broad-spectrum drugs also presenting better tolerability and less toxicity must be developed to achieve the definitive cure.<sup>9</sup>

A major approach to increase the efficacy of bioactive compounds while decreasing toxicity has involved their chemical attachment to synthetic or natural macromolecules.<sup>10–12</sup> Thus, many different polymeric systems have been attached *via* degradable linkages to various therapeutic agents. The original idea is that, in the body, these systems could undergo hydrolytic or enzyme-catalyzed cleavages so that the therapeutic agent is released

**Keywords:** Oxamniquine; Schistosomicide; Polymeric prodrug; Molecular modeling.

\* Corresponding author. Tel.: +55 011 30913793; fax: +55 019 3232 4538; e-mail: [rparisef@usp.br](mailto:rparisef@usp.br)

at a predetermined rate.<sup>13–15</sup> Drugs are, in general, lower molecular weight compounds which rapidly penetrate in several kinds of cells being eliminated right afterward. Higher and repeated doses must be administered to keep the therapeutic effect and favor adverse effects.<sup>16</sup> With the purpose of obtaining new and better oxamniquine derivatives, polymeric prodrugs have been planned. Methacrylic and acrylic monomers were selected as carriers. Polymethacrylic and polyacrylic are known to anchor drugs,<sup>17–20</sup> promoting improved bioavailability, prolonged action, and reduced adverse effects.<sup>10,21–23</sup> The numerous free carboxyl groups presented in these polymers allow ester or amide linkages to be easily obtained. The final products are characterized to be bio-stabilized polymers, by not causing immunogenicity, being easily eliminated, and having low toxicity.<sup>24</sup>

## 2. Results and discussion

### 2.1. Synthesis

Compounds **1** and **2** were obtained by treatment of oxamniquine with methacrylic and acrylic acids, respectively. These were submitted to polymerization reactions but only the methacrylic copolymer **3** was obtained. Figure 1 shows the corresponding chemical structures.

The esterification reaction of oxamniquine using DCC and DMAP<sup>25</sup> proved to be an effective method to obtain the methacrylic monomer (**1**). This was characterized specially by the singlet, at 1.95 ppm, corresponding to the methylic protons and two other singlets, at 6.11 and 5.57 related to the vinylic protons, both from the methacrylic species. The signal of the CH<sub>2</sub> protons (H-16) shifted from 4.69 ppm to 5.37 ppm, when compared to oxamniquine (data not shown). This shift also may characterize the linkage between the monomer and the drug. This hypothesis was corroborated by the <sup>13</sup>C NMR spectrum, in which the appearance of a signal at 18.7 ppm, characteristic of vinylic methyl group, was observed. At 167.5 ppm, a typical signal of the carbonyl group was noted, confirming the ester linkage. The elemental analysis and melting point confirm the structural formula and the high degree of purity. It is interesting to note that the reaction between the oxamniquine and methacrylic acid, using Sheehan and Hess method,<sup>26</sup> results in the proposed monomer by an ester linkage. A similar product was expected in the reaction using the acrylic acid. However, the oxamniquine acrylate was not obtained.

A new methodology described by Mank<sup>27</sup> was applied and an unexpected oxamniquine acrylamide compound (**2**) was obtained. Mank's methodology<sup>27</sup> is a well-known procedure named phase transfer reactions. The reaction medium favored the purification, allowing a higher degree of purity confirmed by both the melting point and elemental analysis. The <sup>1</sup>H NMR spectrum showed three signals at 6.64 ppm (H-18), 6.36 ppm (H-19) and 5.75 ppm (H-19'), related to the vinylic protons of the acryloyl species. A shift from 2.81 ppm (H-13) in oxamniquine to 4.24 ppm (H-13) characterizes the link-

age of an acyl group in the nitrogen atom (H-12) of the side chain. These results were confirmed in <sup>13</sup>C NMR spectroscopy by the occurrence of a special signal at 169.1 ppm, typical of the carbonyl group of an amide.

The compounds **1** and **2** were submitted to radical polymerization followed by copolymerization reactions.<sup>28</sup> However, only the oxamniquine methacrylic copolymer (**3**) was obtained. The low solubility in common solvents hindered its characterization by NMR. Nevertheless, extensive thermal and infrared analyses indicate the formation and purity of this compound.<sup>25</sup> The calculated substitution grade is in agreement with the synthetic method (Compound **1**—1 mmol and methacrylic acid—2 mmol). The corresponding acrylic copolymer was not obtained, as acrylamide polymerizations usually require more drastic conditions<sup>29</sup> which could lead to oxamniquine degradation.

### 2.2. Molecular modeling

The molecular modeling study was performed in order to assist the elucidation of the reactivity of oxamniquine and its distinct behavior in the acylation reactions with methacrylic and acrylic acids, as reported in the synthesis section. To contribute to this purpose, an oxamniquine analogue without the nitro group was proposed.

The analysis of the minimal energy conformer of oxamniquine obtained with AM1 suggests that the hydroxybenzyl group would be orientated in the direction of that nitro, as it can be seen in Figure 2, at space-filling (Corry–Pauling–Koltun) model. This orientation may result from a hydrogen bond involving the hydroxyl hydrogen (hydrogen-bond donor) and an oxygen atom (hydrogen-bond acceptors) of the nitro group. The visual observation can be supported by the analysis of the distances between the referred atoms (O–H·····O–NO) of 2.2 Å. As we know it, hydrogen bonds are attractive inter- or intra-molecular interactions of common occurrence when oxygen, nitrogen or fluorine atoms meet near a hydrogen atom, also attached to one of these electronegative elements.<sup>30</sup> Hydrogen bonds occur in intervals from 2 to 3 Å, which fulfills the distance here observed. Once formed, the hydrogen bond will stabilize the hydroxybenzyl group, decreasing its reactivity. In comparison, the hydroxybenzyl group of the nitro-lacking analogue is shown in a different and free orientation (Fig. 2).

The hydrogen bond hypothesis may be corroborated by the MEPs' analysis of oxamniquine and its analogue (Fig. 2). A higher electronic density (weak blue color) is observed near the region of the hydroxyl hydrogen of oxamniquine compared to that on the nitro-lacking analogue (more intense blue color). This relative superior electronic density may be associated with a lower acidity of this alcoholic group on oxamniquine. In addition, the MEPs analyses also suggest that the nucleophilicity of the hydroxyl oxygen on oxamniquine may also be decreased due to its resonance donor effect toward the heterocyclic system. This one would be electronically disfavored by the strong acceptor nature of the nitro group. A red-orange continuous area starts

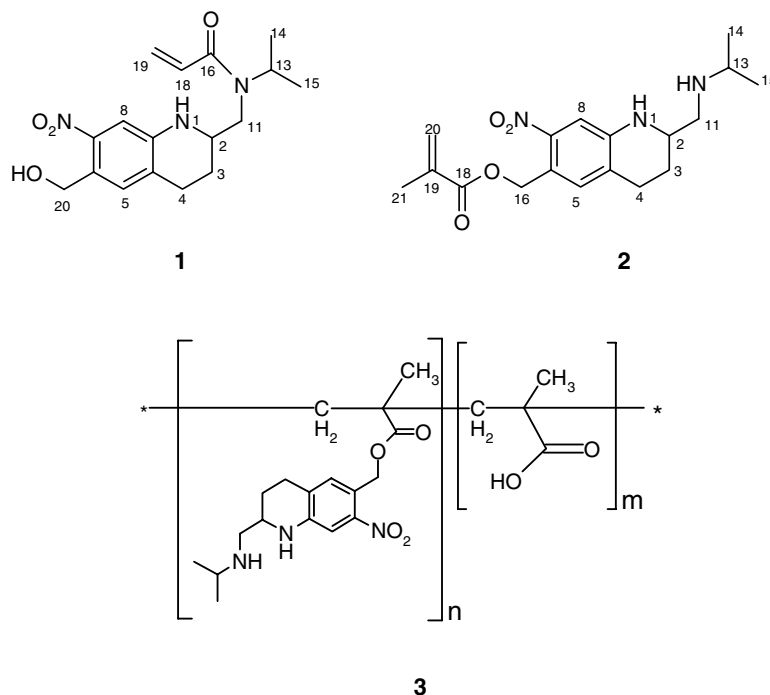


Figure 1. Chemical structures of oxamniquine prodrugs.

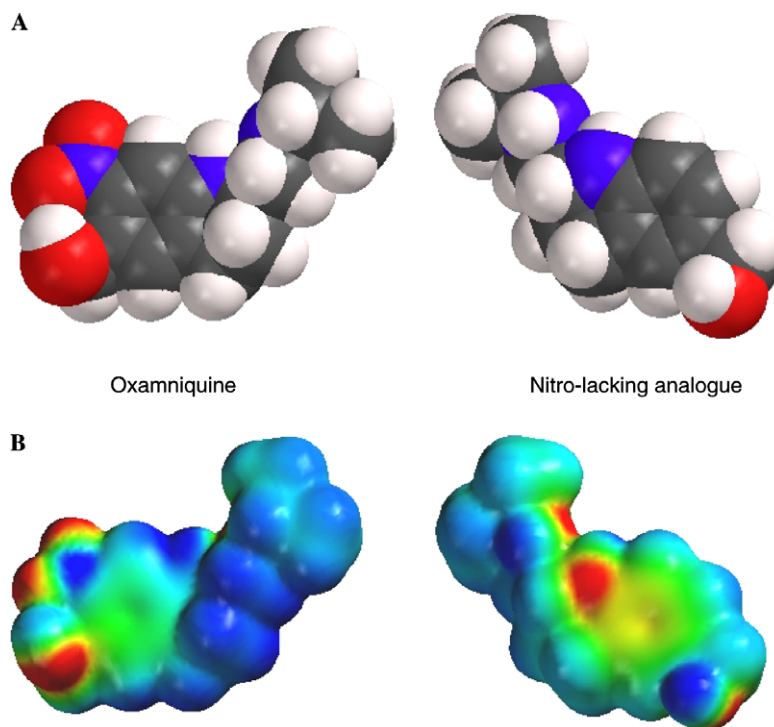


Figure 2. Anterior and posterior faces of the minimal energy conformers of oxamniquine and its nitro-lacking analogue at space-filling model. On the same orientations are shown the respective electrostatic potential maps (B), in the range from  $-50$  (deepest red) to  $+20$  (deepest blue) kcal/mol. Atom color code: C (gray), O (red), N (blue), and H (white).

from the hydroxyl oxygen atom in the direction of the oxamniquine aromatic nucleus. In opposition, the correspondent nucleus in the nitro-lacking analogue shows a richer electronic density represented by a greater and more intense orange color. It is important to note that the hydrogen bond observation was first reported for

oxamniquine and may be considered relevant to comprehending its chemical reactivity as well as to explain synthetic difficulties.

The analysis of the MEPs of the *s-cis* configuration of the methacrylic and acrylic acids calculated with

3-21G\* method (Fig. 3) indicates, as expected, a lower electronic density near the region of the carbonyl carbon (more intense blue color). This can be attributed to the presence of electronegative carboxylic oxygen atoms, highly electron-rich centers (showed by the orange-red color map). Nevertheless, the nature of the unsaturated carbon, in particular the first  $sp^2$  carbon adjacent to the carbonyl carbon, seems to lead to a small but distinctive electronic character between both acids. The nonsubstituted unsaturated carbon of the acrylic acid allows a greater electron delocalization between the carbonyl carbon and those of the allylic bond. This observation is symbolized by an extended blue color over the referred carbon atoms. Concerning the methacrylic acid, the presence of the methyl group disfavors this resonance effect, concentrating the electron deficiency over the carbonyl carbon. These observations are corroborated by the LUMO maps which indicate a relatively higher concentration of the most electron-deficient area (blue color) over the carbonyl carbon of the methacrylic acid, suggesting this acid to be a better site for nucleophilic attack. These small electronic differences observed between these two acids associated with the decreased nucleophilicity of the benzylic alcohol on oxamniquine, as previously commented, may explain the attainment of the methacrylate compound (**1**) but not of the acrylic one, as observed experimentally.

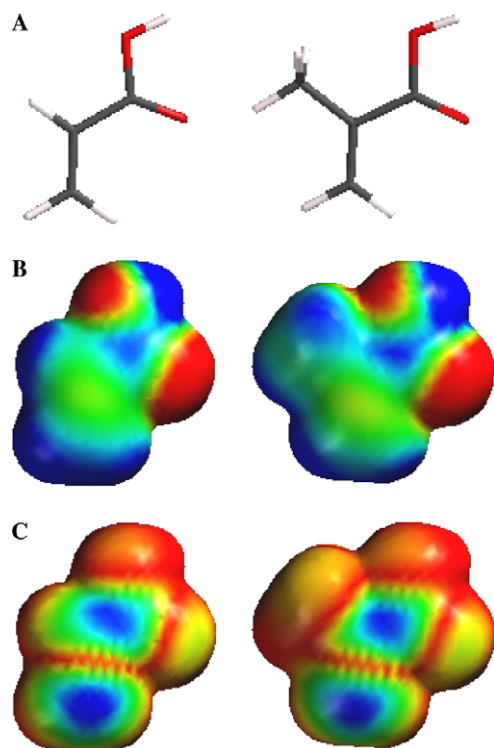


**Figure 3.** Acrylic (left) and methacrylic (right) acids shown at tube model (A). On the same orientation are shown the respective electrostatic potential maps (B) on color bands in the range of  $-25$  (deepest red) to  $+15$  (deepest blue) kcal/mol and LUMO maps (C) in the range from  $0.001$  (deepest red) to  $0.035$  (deepest blue) kcal/mol. Atom color code as named in Figure 2.

It was verified that the reaction between oxamniquine and acrylic acid occurs through an amide linkage (compound **2**). The molecular modeling study using AM1 allows hypothesizing that the acrylamide of oxamniquine might be obtained from the combination of a lower steric hindrance in the approximation and posterior reaction of the secondary nitrogen atom of the drug side chain and the acrylic acid. A highly steric effect, especially observed between the isopropyl group of oxamniquine and the methyl group of methacrylic acid, would disfavor the correspondent methacrylamide compound. This hypothesis can be visualized by the manual atomic superposition of the minimal energy conformers (Fig. 4) of the oxamniquine acrylamide (**2**) and the hypothesized methacrylamide.

### 2.3. Biological evaluation

Preliminary biological screening aims to evaluate the activity of the compounds **1**, **2**, and **3**, and to compare the prolonged action, especially for the methacrylic copolymer, in relation to oxamniquine. The *in vivo* assays were carried out using the quantitative oogram test and the mesenteric veins perfusion technique.<sup>31,32</sup>

In the quantitative oogram test, two aspects were considered to indicate the event of biological activity:

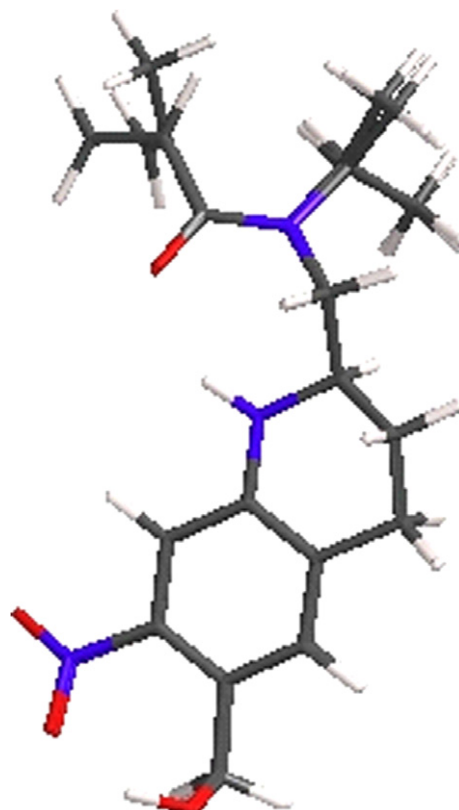


**Figure 4.** Manual superposition of the minimal energy conformers of oxamniquine acrylamide (**2**) (upper) and the hypothesized methacrylamide compound taking as references the atoms of the 1,2,3,4-tetrahydro-2-aminomethyl-7-nitro-6-quinolinomethanol system. Atom color code as named in Figure 2.

oviposition suppression and the increase of the immature number of eggs. The suppression of the number of eggs may be related to the death of male and female parasites, the death of just one sex, or yet the activity of the drug over the reproduction system of the male or female worms. First, the evaluation of the egg maturity stage would verify the direct action over the parasite life cycle, so that the potency of the compound is shown. Second, it can indicate the direct action over the eggs, so the biological effect is also shown. Therefore, the compounds were evaluated over the 1st, 2nd, and 3rd stages of the eggs. The results obtained from the quantitative oogram test are presented in Table 1. The oxamniquine methacrylate and the acrylamide, groups 1 and 2, respectively, showed a decrease in the number of eggs compared to the untreated group, so that antiparasitic activity may be associated. Oxamniquine polymethacrylate, group 3, provided a decrease in the number of eggs, particularly in the 1st and 2nd stages (20th day). However, this effect cannot be considered enough to treat the animals.

In addition to the oogram test, the mesenteric veins perfusion technique allowed to evaluate the action stage, that is, if the compound acts directly toward the worm or if, at the experimental period, only the reproductive system has been affected. It is recognized that, a high number of worms associated with a low number of eggs indicate the first activity against the reproductive system. Conversely, a low number of worms and eggs indicate that the viability of the worms has been affected. Table 2 shows the distribution of the total number of worms in relation to the 10th and 20th days of infection

compared with the untreated group. As in the oogram test, the oxamniquine methacrylate, group 1, (in particular) and the acrylamide compound, group 2, also showed a decrease in the number of worms. The same was observed in oxamniquine. Its corresponding methacrylate copolymer (group 3) did not affect the number of worms until the 10<sup>th</sup> day, data similar to the untreated group, and showed a fairly significant decrease in the 20<sup>th</sup>, as observed in relation to the number of eggs.

## 2.4. Statistical analysis

In the statistical analysis, assessing the hypothesis H is the main interest:  $\lambda = 1$  ( $\mu_U = \mu_T$ ) against A:  $\lambda \neq 1$  ( $\mu_U \neq \mu_T$ ), under a significance level of 5%. Then, 95% exact interval estimates for the ratio  $\lambda$  are performed for each compound. Table 2 describes the maximum likelihood (ML) estimates as well as 95% exact interval estimates for  $\lambda$  for all compounds studied. A strong evidence appears against the null hypothesis H for oxamniquine (10th and 20th days) and compounds 1 and 2 (10th and 20th days) for which the exact interval estimates do not cover the null hypothesis value of  $\lambda$ . These results show the clear superiority of the treated groups, which have a smaller number of worms than the untreated group. In all these cases, the  $p$  value is inferior to 0.05. For instance, the ML estimate of  $\lambda$  for oxamniquine equals 47.67 (10th day), and 12.00 (20th day) with the corresponding exact interval estimates given by [16.05, 232.01] and [6.84, 22.84], respectively. For 1 and 2, the ML estimates of  $\lambda$  are, respectively, 7.09 and 2.43 (10th day) and 15.89 and 3.67 (20th day). However, for the remaining case of oxamniquine methacrylate

**Table 1.** Average of eggs according to the quantitative oogram test

Group	Average of eggs					
	10th day stage			20th day stage		
	1°	2°	3°	1°	2°	3°
Untreated	14.2	13.1	25.1	N/D	N/D	N/D
1	0	0.08	0.16	0	0.09	0.27
2	0	0.11	0.22	0	0.09	0.27
3	15.27	14.72	16.18	7.11	9.33	20
Oxamniquine	0	0	0	0	0	0

N/D, not determined.

**Table 2.** Distribution of the total number of worms in relation to the 10th and 20th days and the ML estimates with the correspondent 95% exact interval estimate

Compound	Period (days)	Number of worms	Number of animals	ML estimate and 95% exact interval estimate for the ratio $\lambda$
Oxamniquine	10	3	11	47.67 [16.05, 232.01]
	20	13	12	12.00 [6.84, 22.84]
1	10	22	12	7.09 [4.54, 11.53]
	20	9	11	15.89 [8.19, 35.11]
2	10	48	9	2.43 [1.76, 3.40]
	20	39	11	3.67 [2.58, 5.29]
3	10	183	11	0.78 [0.63, 0.96]
	20	125	9	0.94 [0.74, 1.18]

Untreated group: number of worms, 182; number of animals, 14.



copolymer (**3**), the statistical test does not detect a difference between treated and untreated groups in the 10th day, but rejects the null hypothesis, under a 5% significance level, in the 20th day. Here, in contrast with the cases of compounds **1** and **2**, the untreated group seems to have a smaller number of worms than that in the treated group.

### 3. Conclusions

New prodrug compounds of oxamniquine were designed and synthesized. Methacrylate (**1**) and acrylamide (**2**) monomers were achieved in good yields although only the methacrylate copolymer (**3**) was possible to obtain. Stereoelectronic features of oxamniquine and of the methacrylic and acrylic acids, as illustrated by the molecular modeling study, may be responsible for these data.

Preliminary in vivo evaluation corroborated by statistical analysis showed that compounds **1** and **2** have prolonged action profile and reduced worm charge. Concerning parasite charge, similar profiles to oxamniquine were observed. Complementary bioassays such as toxicological test will be important to the major evaluation of these prodrugs. Otherwise, for compound **3**, a significant increase in the number of worms was observed suggesting that the methacrylate copolymer did not exhibit antiparasitic activity. This behavior may be related to several factors such as: (1) The polymer is a prolonged release form, thus the compound might not have achieved the effective dose in the studied period. A longer experimental period would be necessary to evaluate this hypothesis; (2) Problems of drug release from the polymeric matrix, in which difficulties in hydrolysis may have interfered in the drug release. Possibly, the introduction of a spacer group between the drug and the polymer could have solved this problem; (3) High molecular weight. Although it was not possible to determine the molecular weight of **3**, its high molecular weight may have inhibited endocytosis process.

## 4. Experimental

### 4.1. Synthesis

Melting points were taken with Microquímica MQAPF 301. NMR spectra were recorded using a Bruker AC-300 Spectrometer at 300 MHz ( $^1\text{H}$ ) and 75 MHz ( $^{13}\text{C}$ ) with tetramethylsilane as internal reference and  $\text{DMSO}-d_6$  as solvent. Chemical shifts are given in ppm (parts per million), coupling constants in Hertz, and splitting patterns are designated as follows: s, singlet; br s, broad singlet; d, doublet; t, triplet; q, quartet, and m, multiplet. The ultraviolet (UV) spectra were recorded on a UV/VIS Beckman DU-70 spectrometer. Elemental analysis (C, H and N) was performed on a Perkin-Elmer 2400.

**4.1.1. Oxamniquine methacrylate (1).** In a round-bottomed flask, oxamniquine (1 mmol) was dissolved in

dichloromethane (60 mL). Methacrylic acid (3 mmol) was added, followed by dimethylaminopyridine (DMAP) (0.5 mmol) and dicyclohexylcarbodiimide (DCC) (6 mmol). The reaction mixture was stirred for 8 h at room temperature.<sup>26</sup> The solution was filtered and evaporated to dryness under reduced pressure. The residue was purified by column chromatography using ethyl acetate/methanol (7:3), yielding 69% of a product with melting point of 66 °C.<sup>25</sup>  $^1\text{H}$  NMR ( $\text{DMSO}-d_6$ , 300 MHz,  $\delta$ =ppm,  $J$  = Hz): 1.10 (d, 3H, H-14,  $J$  = 6.7); 1.12 (d, 3H, H-15,  $J$  = 6.7); 1.52–1.58 (m, 1H, H-3'); 1.95 (s, 3H, H-21); 1.91–1.98 (m, 1H, H-3); 2.51 (t, 1H, H-11',  $J$  = 6.7); 2.72–2.80 (m, 3H, H-4 and H-13); 2.88–2.93 (m, 1H, H-11); 3.36 (m, 1H, H-2); 5.37 (s, 2H, H-16); 5.57 (br s, 1H, H-19'); 6.11 (br s, 1H, H-19); 7.03 (s, 1H, H-5); 7.20 (s, 1H, H-8).  $^{13}\text{C}$  NMR ( $\text{DMSO}-d_6$ , 75 MHz,  $\delta$ =ppm) 18.7 ( $\text{C}_{21}$ ), 22.9 ( $\text{C}_{14}$ ); 23.5 ( $\text{C}_{15}$ ); 26.0 ( $\text{C}_3$ ); 26.8 ( $\text{C}_4$ ); 49.5 ( $\text{C}_{13}$ ); 51.3 ( $\text{C}_{11}$ ); 52.7 ( $\text{C}_2$ ); 64.0 ( $\text{C}_{16}$ ); 109.6 ( $\text{C}_8$ ); 118.5 ( $\text{C}_6$ ); 126.3 ( $\text{C}_{20}$ ); 131.4 ( $\text{C}_5$ ); 136.5 ( $\text{C}_{19}$ ); 145.3 ( $\text{C}_7$ ); 147.4 ( $\text{C}_9$ ); 163.0 ( $\text{C}_{10}$ ); 167.5 ( $\text{C}_{18}$ ). Elemental analysis showed that, to the molecular formula of  $\text{C}_{18}\text{H}_{25}\text{N}_3\text{O}_4$ , the following values were observed: C 61.89% (62.23); H 7.08% (7.25); and N 11.94% (12.09). The respective theoretical values are in parentheses.

**4.1.2. Oxamniquine acrylamide (2).** In a round-bottomed flask, equipped with a dropping funnel, oxamniquine (1.1 mmol), sodium bicarbonate (119 mmol), and water (30 mL) were added. This mixture was kept in an ice bath, and a solution of acryloyl chloride in dichloromethane (1 mmol: 10 mL) was added, over 1 h. The mixture was stirred for 50 min at room temperature and allowed to sit undisturbed for 20 min without stirring.<sup>27,33</sup> The organic phase was transferred to a separatory funnel and washed three times with 20 mL of water. The organic phase was dried over anhydrous sodium sulfate and the solvent was removed. The residue was submitted to column chromatography using ethyl acetate/methanol (7:3), yielding 52% of a product with melting point of 109 °C.  $^1\text{H}$  NMR ( $\text{DMSO}-d_6$ , 300 MHz,  $\delta$ =ppm,  $J$  = Hz): 1.22 (d, 3H, H-15,  $J$  = 6.7); 1.25 (d, 3H, H-14,  $J$  = 6.7); 1.68 (m, 1H, H-3'); 1.95 (m, 1H, H-3); 2.82 (m, 2H, H-4); 3.25 (t, 1H, H-11',  $J$  = 10.5); 3.54 (m, 1H, H-2); 3.55 (m, 1H, H-11); 4.24 (m, 1H, H-13); 4.69 (s, 2H, H-20); 5.75 (d, 1H, H-19',  $J$  = 10.3); 6.36 (d, 1H, H-19,  $J$  = 16.7); 6.64 (dd, 1H, H-18,  $J_{\text{cis}}$  = 10.3,  $J_{\text{trans}}$  = 16.7); 7.20 (s, 1H, H-5); 7.21 (s, 1H, H-8);  $^{13}\text{C}$  NMR ( $\text{DMSO}-d_6$ , 75 MHz,  $\delta$ =ppm) 22.0 ( $\text{C}_{15}$ ); 21.7 ( $\text{C}_{14}$ ); 26.2 ( $\text{C}_3$ ); 26.8 ( $\text{C}_4$ ); 47.8 ( $\text{C}_{11}$ ); 49.6 ( $\text{C}_{13}$ ); 53.6 ( $\text{C}_2$ ); 63.2 ( $\text{C}_{20}$ ); 109.9 ( $\text{C}_8$ ); 123.9 ( $\text{C}_6$ ); 127.1 ( $\text{C}_{10}$ ); 128.6 ( $\text{C}_{19}$ ); 128.7 ( $\text{C}_{18}$ ); 131.9 ( $\text{C}_5$ ); 144.9 ( $\text{C}_7$ ); 147.3 ( $\text{C}_9$ ); 169.1 ( $\text{C}_{16}$ ). Elemental analysis showed that, to the molecular formula of  $\text{C}_{17}\text{H}_{23}\text{N}_3\text{O}_4$ , the following values were observed: C 61.28% (61.24); H 7.09% (6.97) and N 12.28% (12.60). The respective theoretical values are in parentheses.

**4.1.3. Oxamniquine methacrylate copolymer (3).** In a glass vial, oxamniquine methacrylate (**1**) (1 mmol) and methacrylic acid (2 mmol) were dissolved in dimethylformamide (1.0 mL). The mixture was stirred and azobisisobutyronitrile (AIBN) 0.5% was added. The glass

vial was sealed under nitrogen atmosphere. The copolymerization was carried out at 50–60 °C for 16 h. The copolymer was precipitated with an excess of diethyl ether.<sup>28</sup> The residue was washed three times with 20 mL of diethyl ether and dried under reduced pressure. The degree of substitution determined by UV was 50.2%. Thermal analysis and infrared spectroscopy characterized the copolymer.<sup>25</sup>

## 4.2. Molecular modeling

The molecular modeling study was performed using Spartan'02 for Linux, version 119a (Wavefunction Inc.). The MMFF94 force field<sup>34</sup> was employed to construct the chemical structures.

**4.2.1. Oxamniquine and its nitro-lacking analogue.** The Hamiltonian Austin Model 1 (AM1)<sup>35</sup> was chosen to model oxamniquine. This semi-empirical method has made superior predictions about conformations,<sup>36</sup> reproducing electrochemical behavior,<sup>37</sup> and fitting experimental heats of formation<sup>38,39</sup> to nitro compounds. After complete geometry optimization of oxamniquine, and in order to better evaluate the conformational feature, systematic analysis was performed at step size of 15° for dihedral angles of the side chain and at steps of 120° for the C<sub>2</sub> and C<sub>3</sub> atoms of the piperidine ring. The minimal energy conformer obtained had the dihedral angle of the hydroxybenzyl group submitted to systematic analysis at step size of 15°. The resulting minimal energy conformation was adopted for oxamniquine. In addition, with the purpose of better estimating the reactivity of oxamniquine, a nitro-lacking analogue compound was designed by elimination of the nitro group from the selected conformer of oxamniquine. A new systematic analysis involving the dihedral angle of the hydroxybenzyl group was followed. The conformer pointed as the minimal energy was adopted. The two selected conformers had their stereo properties and electronic surfaces evaluated according to the single point calculation. Maps of the molecular electrostatic potential (MEPs) showing the total electron density surface were also calculated. In this work, the MEPs' isoenery contour was generated in a –45 to +20 kcal/mol range and superimposed onto a surface of constant electron density of 0.002 e/au<sup>3</sup>. The constants employed in these calculations are default parameters in Spartan.

**4.2.2. Methacrylic and acrylic acids.** In order to better estimate the electronic properties of the methacrylic and acrylic acids, an ab initio 3-21G\* calculation was performed. After geometry optimization, the conformational analysis proceeded according to the systematic search with the respective dihedral angles (C=C–C=O) rotated at step size of 15°. The *s-cis* configuration was pointed out for both minimal energy conformers which were then submitted to a single point calculation. MEPs and LUMO maps were generated in a –25 to +15 kcal/mol and 0.001–0.035 kcal/mol range, respectively. The LUMO maps illustrate the absolute value of the lowest unoccupied molecular orbital onto the total electron density surface. Surfaces of constant electron density of 0.002 e/au<sup>3</sup> for MEPs and isosurfaces

at 0.0032 au for LUMO maps were employed as default parameters in Spartan.

**4.2.3. Oxamniquine acrylamide and its methacrylamide compound.** To also elucidate the oxamniquine reactivity in relation to the acrylic and methacrylic acids, the oxamniquine acrylamide (**2**) and the hypothesized methacrylamide compound were designed. The AM1 basis set was employed. Starting from the adopted minimal energy conformer of oxamniquine, the optimized geometries of the amides were submitted to systematic analysis having the dihedral angles near the amide linkage rotated at step size of 15°. The respective minimal energy conformers were then selected.

## 4.3. In vivo biological tests

The biological evaluation was performed on male 'Swiss' mice, weighing 30–40 g, infected subcutaneously with 50 *S. mansoni* BH strain cercariae. For infection confirmation, fecal analysis by the direct egg method was carried out 45 days after inoculation. The presence of just one egg indicates the infection. The positive mice were trialed and separated. The negative ones were submitted for further examination and persisting negative were eliminated. The infected mice were distributed in six groups of 15 animals and a solution of 15% Cremophor® EL in water was used as a vehicle. The groups were defined: untreated group; vehicle group; oxamniquine group—oxamniquine 50 mg/kg; Group 1—oxamniquine methacrylate (**1**); Group 2—oxamniquine acrylamide (**2**), and Group 3—oxamniquine methacrylate copolymer (**3**).

Each compound was suspended in the vehicle solution, administered per os, in a single dose, by gastric sound, at 50 mg/kg weight. The animals were sacrificed after 10- and 20-day treatment.

The method of perfusion of the mesenteric and portal veins was employed to quantify adult worms. From each mouse, two thin gut fragments (about 1 cm) were removed to verify the number of eggs and also the stages of development (quantitative oogram method).<sup>31,32</sup>

## 4.4. Statistical analysis

In the statistical analysis it was assumed, for each group, that the total number of worms denoted by  $W$  follows a Poisson distribution with mean  $n\mu$ , namely  $W \sim P(n\mu)$ , in which  $\mu$  is the expected number of worms per animal and  $n$  is the number of animals. The parameter of interest is the ratio  $\lambda = \mu_U/\mu_T$ , in which  $\mu_U$  and  $\mu_T$  denote, respectively, the expected number of worms in the untreated and treated groups. In order to perform exact inferences for the parameter of interest  $\lambda$ , a conditional distribution of the total number of worms of the untreated group, named  $W_U$ , in relation to the total number of worms of the two groups was named  $m = W_U + W_T$ . This is a binomial distribution of probability  $\pi$  and  $m$  assays, where  $\pi = \lambda n_U/(n_T + \lambda n_U)$  with  $n_U$  and  $n_T$  denoting, respectively, the number of animals in the untreated and treated groups (see, e.g., Ref. 40).

Finally, exact inferences for  $\lambda$  can be performed using the approach given in Leemis and Trivedi.<sup>41</sup>

### Acknowledgments

The authors acknowledge Pfizer for providing oxamni-quine, Conselho Nacional de Desenvolvimento Científico e Tecnológico (CNPq), Fundação de Amparo à Pesquisa do Estado de São Paulo (FAPESP) (Processo 01/09744-5), and the Coordenação de Aperfeiçoamento de Pessoal de Nível Superior (CAPES)—Programa ProDoc (Processo 00019-03-8) for financial support.

### References and notes

- World Web site <http://www.who.int/ctd/schistourlhttp://www.who.int/ctd/schisto>.
- Schistosomiasis. *Bull. World Health Organ.* **1988**, 76, 150.
- Sparg, S. G.; Van-Staden, J.; Jager, A. K. *J. Ethnopharmacol.* **2000**, 73, 209.
- Ferreira, H. S.; Coutinho, E. M. *Ann. Trop. Med. Parasitol.* **1999**, 93, 437.
- Cioli, D. *Parasitol. Today* **1998**, 14, 418.
- Coura, J. R. *Mem. Inst. Oswaldo Cruz* **1995**, 90, 257.
- Cioli, D.; Pica-Mattoccia, L.; Archer, S. *Pharmacol. Ther.* **1995**, 68, 35.
- Shekar, K. C. *Drugs* **1991**, 42, 379.
- Parise-Filho, R.; Silveira, M. A. B. *Rev. Bras. Cienc. Farm.* **2001**, 37, 123.
- Ouchi, T.; Ohya, Y. *Prog. Polym. Sci.* **1995**, 20, 211.
- Patel, H.; Raval, D. A.; Madanwar, D. *Angew. Makromol. Chem.* **1997**, 245, 1.
- Ringsdorf, H. *J. Polym. Sci.* **1975**, 51, 135.
- Bundgaard, H., Ed.; *Design of Prodrugs*; 1985, Elsevier Science: Amsterdam, p 360.
- Chung, M. C.; Ferreira, E. I. *Quím. Nova* **1999**, 22, 75.
- Friis, G. J.; Bundgaard, H. Design and Application of Prodrugs. Krogsgaard-Larsen, P., Liljefors, T., Madsen, T., Eds; In *A Textbook of Drug Design and Development*, 2nd ed.; 1996, Hardwood Academic: Amsterdam, pp 351–385.
- Kalcic, I.; Zorc, B.; Butula, I. *Int. J. Pharm.* **1996**, 136, 31.
- Erdmann, L.; Uhrich, K. E. *Biomaterials* **2000**, 21, 1941.
- Etrych, T.; Jelínková, M.; Ríhová, B.; Ulbrich, K. *J. Control. Release* **2001**, 73, 89.
- Gallardo, A.; Fernández, F.; Cifuentes, A.; Díez-Masa, J. C.; Bermejo, P.; Rebuelta, M.; López-Bravo, A.; San Román, J. *J. Control. Release* **2001**, 72, 1.
- Jiang, H. L.; Zhu, K. J. *Biomaterials* **2001**, 22, 211.
- Davaran, S.; Entezami, A. A. *J. Control. Release* **1997**, 47, 41.
- Wermuth, C. G., Ed.; In *The Practice of Medicinal Chemistry*; 1996, Academic: London, pp 697–716.
- Yura, H.; Yoshimura, N.; Hamashima, T. *Transplant Proc.* **1998**, 30, 3598.
- Soyez, H.; Schacht, E.; Vanderkerden, S. *Adv. Drug Delivery Rev.* **1996**, 21, 81.
- Parise-Filho, R.; Araújo, A. A. S.; Santos-Filho, M.; Matos, J. R.; Silveira, M. A. B. *J. Therm. Anal. Cal.* **2004**, 75, 487.
- Sheehan, J. C.; Hess, G. P. *J. Am. Chem. Soc.* **1955**, 77, 1067.
- Mank, R.; Kala, H.; Strube, M. *Pharmazie* **1988**, 43, 692.
- San Román, J.; Madruga, E. L. *Polymer* **1989**, 30, 949.
- Sandler, S. R.; Karo, W. *Polymer Synthesis*, 2nd ed.; In *Organic Chemistry*; Wasserman, H. H., Ed.; Academic: San Diego, 1992; Vol. 29-I, pp 559–560.
- Erickson, J. A.; McLoughlin, J. I. *J. Org. Chem.* **1995**, 60, 1626.
- Pellegrino, J.; Faria, J. *Am. J. Trop. Med. Hyg.* **1965**, 14, 363.
- Pellegrino, J.; Siqueira, A. F. *Rev. Bras. Malariol. Doenças Trop.* **1956**, 8, 589.
- Drobník, J.; Kopeček, J.; Labský, J.; Rejmanová, P.; Exner, J.; Saudek, V.; Kálal, J. *Makromol. Chem.* **1976**, 177, 2833.
- Halgren, T. A. *J. Comput. Chem.* **1996**, 17, 490.
- Dewar, M. J. S.; Zebisch, E. G.; Heally, E. F.; Stewart, J. J. P. *J. Am. Chem. Soc.* **1985**, 107, 3902.
- Debnath, A. K.; Lopez de Compadre, R. L.; Debnath, G.; Shusterman, A. J.; Hansch, C. *J. Med. Chem.* **1991**, 34, 786.
- Lehmann, M. W.; Singh, P.; Evans, D. H. *J. Electroanal. Chem.* **2003**, 549, 137.
- Chen, C.; Wu, J. C. *Comput. Chem.* **2001**, 25, 117.
- Chen, P. C.; Wu, J. C.; Chen, S. C. *Comput. Chem.* **2001**, 25, 439.
- Breslow, N. E.; Day, N. E. International Agency for Cancer Research, IARC Scientific Publications: Lyon, n. 82, 1987.
- Leemis, L. M.; Trivedi, K. S. *Am. Statist.* **1996**, 50, 63.